J|A|C|S
ARTICLES
Published on Web 09/21/2004

Catalytic Nanomotors: Autonomous Movement of Striped Nanorods

Walter F. Paxton,[†] Kevin C. Kistler,[†] Christine C. Olmeda,[†] Ayusman Sen,*[,†] Sarah K. St. Angelo,[†] Yanyan Cao,[†] Thomas E. Mallouk,*[,†] Paul E. Lammert,[‡] and Vincent H. Crespi*[,‡]

Contribution from the Departments of Chemistry and Physics, The Pennsylvania State University, University Park, Pennsylvania 16802

Received April 21, 2004; E-mail: asen@psu.edu; tom@chem.psu.edu; crespi@phys.psu.edu

Abstract: Rod-shaped particles, 370 nm in diameter and consisting of 1 μm long Pt and Au segments, move autonomously in aqueous hydrogen peroxide solutions by catalyzing the formation of oxygen at the Pt end. In 2−3% hydrogen peroxide solution, these rods move predominantly along their axis in the direction of the Pt end at speeds of up to 10 body lengths per second. The dimensions of the rods and their speeds are similar to those of multiflagellar bacteria. The force along the rod axis, which is on the order of 10^{-14} N, is generated by the oxygen concentration gradient, which in turn produces an interfacial tension force that balances the drag force at steady state. By solving the convection-diffusion equation in the frame of the moving rod, it was found that the interfacial tension force scales approximately as $SR^2\gamma/\mu DL$, where S is the area-normalized oxygen evolution rate, γ is the liquid−vapor interfacial tension, R is the rod radius, μ is the viscosity, D is the diffusion coefficient of oxygen, and L is the length of the rod. Experiments in ethanol−water solutions confirmed that the velocity depends linearly with the product $S\gamma$, and scaling experiments showed a strong dependence of the velocity on R and L. The direction of motion implies that the gold surface is hydrophobic under the conditions of the experiment. Tapping-mode AFM images of rods in air-saturated water show soft features that are not apparent in images acquired in air. These features are postulated to be nanobubbles, which if present in hydrogen peroxide solutions, would account for the observed direction of motion.

Introduction

The creation of miniature "engines" that can convert stored chemical energy to motion is one of the great remaining challenges of nanotechnology. Nanoscale motors are ubiquitous in biology, and operate by enzymatic catalysis of spontaneous reactions, such as the hydrolysis of ATP and GTP.[1,2] Such motors do not require input of power from macroscopic external circuits or other devices, and are therefore of much current interest in the design of micromechanical systems. Apart from biological and "hybrid" systems that contain enzymatic components, however, the principle of catalytic conversion of chemical to mechanical energy has not been demonstrated with nanoscale and micron-sized objects. Here we report the autonomous, non-Brownian movement of platinum/gold (Pt/Au) nanorods with spatially defined zones that catalyze the spontaneous decomposition of hydrogen peroxide in aqueous solutions.

Whitesides and co-workers have used the catalytic decomposition of hydrogen peroxide to propel cm/mm-scale objects on a water surface.[3] In that case, movement could be attributed to the recoil force of the oxygen (O_2) bubbles released from the Pt catalyst, which was situated on only one side of the "transom" of the "boat." While our initial expectation was that a similar propulsion mechanism would be operative in the case of Pt/Au nanorods, we found that movement occurred in the *opposite* direction, namely toward the platinum end of the rod. Moreover, macroscopic bubbles did not nucleate selectively at the Pt ends of the rods in the reaction, and the motion of the rods did not appear to be connected with the release of bubbles from either end. These observations suggested that a different mechanism is operative on the microscale.

With micron-size objects, interfacial forces can easily be larger than inertial forces, and so we investigated the possibility that motion could be driven by an interfacial tension gradient that is continually re-established by the catalytic reaction as the rod moves through the medium. Rotary surface tension motors in which a mercury drop is driven by electrical energy from an external circuit have already been demonstrated.[4] Interfacial tension also plays an important role in so-called "camphor motors," in which small particles of camphor move at the air−water interface by slowly dissolving and spreading a hydrophobic "wake" behind them.[5] The generation of oxygen at the

[†] Department of Chemistry, The Pennsylvania State University.
[‡] Department of Physics, The Pennsylvania State University.

(1) Soong, R. K.; Bachand, G. D.; Neves, H. P.; Olkhovets, A. G.; Montemagno, C. D. *Science* **2000**, *290*, 1555−1558.
(2) Pantaloni, D.; Le Clainche, C.; Carlier, M.-F. *Science* **2001**, *292*, 1502−1506.
(3) Ismagilov, R. F.; Schwartz, A.; Bowden, N.; Whitesides, G. M. *Angew. Chem., Int. Ed.* **2002**, *41*, 652−654.
(4) Lee, J.; Kim, C.-J. *Proc. IEEE MEMS Workshop* **1998**, *1998*, 538−543.
(5) Nakata, S.; Doi, Y.; Hayashima, Y. *J. Phys. Chem. B* **2002**, *106*, 11681−11684.

10.1021/ja047697z CCC: $27.50

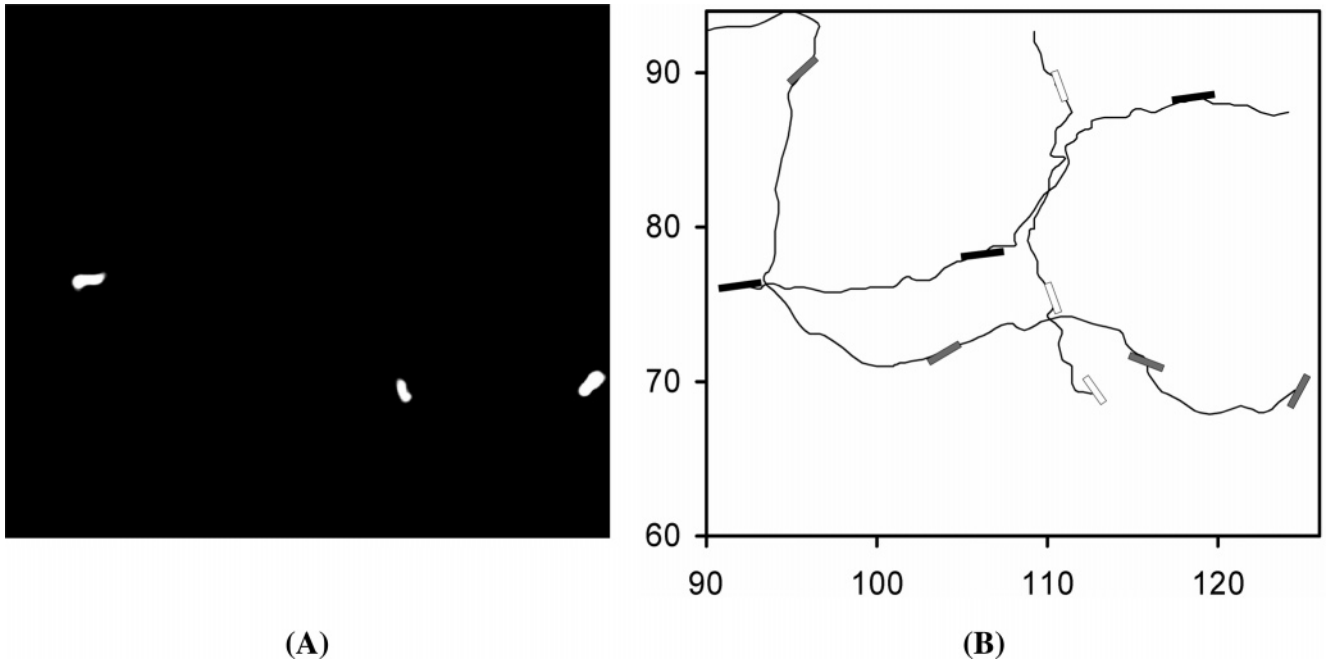

Figure 1. Trajectory plots of three 2 μm long platinum/gold rods identified in (A) over the next 5 seconds. (B) in 2.5% aqueous hydrogen peroxide.

Pt end of the rod disrupts the hydrogen bonding network of water, lowering the liquid−vapor interfacial tension. Because oxygen is generated at only one end, an interfacial tension gradient is created along the length of the rod. As the rod moves, this gradient is continuously reestablished. By solving the convection-diffusion equation in the frame of the moving rod, we show that the interfacial tension force that propels the rod has approximately the same magnitude as the drag force, which is easily calculated from the velocity of the rod. The interfacial tension model thus gives forces of the correct magnitude to explain the observed motion. The direction of motion is more difficult to explain, because it requires that the gold surface is hydrophobic under the conditions of the experiment. We tentatively attribute the hydrophobicity of the gold to nanobubbles that are pinned to its surface, which effectively provide a liquid−vapor interface where the solution meets the rod.

Experimental Section

Striped platinum/gold (Pt/Au) nanorods that are approximately 370 nm in diameter and containing platinum and gold segments, each 1 μm long, were synthesized electrochemically in Anopore alumina membranes and subsequently freed by using a previously reported procedure.[6] Platinum and gold were chosen because platinum is an active hydrogen peroxide decomposition catalyst and gold is not. The rods were characterized by transmission electron and dark-field optical microscopy. In the latter, the gold and the platinum segments were distinguishable due to a difference in color, allowing the direction of motion to be monitored.

A suspension of rods in aqueous hydrogen peroxide was prepared and a known volume (25 μL) of this mixture was placed in a sealed well on a clean glass slide and topped with a glass cover slip. Rods remained suspended in the fluid above the glass slide due to surface charge repulsions between the rods and glass. Diffusion coefficients and rod velocities were determined by analyzing captured video clips of each experiment.

Oxygen evolution rates were determined using suspensions of the same rods that were imaged by video microscopy. An aqueous solution containing 3.7% hydrogen peroxide and a known concentration of Pt/Au rods was placed in a septum-capped tube and the system was purged with argon. The headspace was then sampled at regular intervals and the amount of oxygen evolution was measured by gas chromatography as described elsewhere.[7] For 2 μm long Pt/Au rods, the experimentally determined rate of oxygen evolution from 3.7% hydrogen peroxide was $9.7(4) \times 10^{-16}$ mol O_2/sec per rod. These experiments were repeated in ethanol/water mixtures containing hydrogen peroxide in order to determine the effect of ethanol addition on the rate of the reaction.

Atomic force microscopy (AFM) was used in tapping mode to obtain topography and phase images of Pt/Au nanorods in air and under air-saturated water. Samples were prepared for AFM imaging by shaking the substrate (a glass slide or a silicon wafer) in a mixture of H_2SO_4 (98%) and H_2O_2 (30%) (7:3 in volume) for 2 min. The substrates were rinsed thoroughly with ethanol and high-purity Milli-Q water, and then dried with an argon stream. An aqueous suspension of Au/Pt nanorods (2.0×10^8 rods/mL) was dropped onto the substrate. After evaporating the water at about 60 °C, the sample was rinsed with water and dried with argon again to remove some of the rods. Most of the rods remained on the surface. Tapping-mode AFM (TMAFM) imaging was performed using a MultiMode Scanning Probe Microscope with a NanoScope IIIa controller (Digital Instruments Inc.). Images in air were taken with silicon cantilevers (Molecular Imaging Inc.) with a resonance frequency of around 300 kHz. Images in High-purity Milli-Q water were taken with narrow, thin oxide-sharpened Si_3N_4 cantilevers (Veeco Instruments Inc.). The Si_3N_4 cantilever was modulated at frequencies in the range of 8−10 kHz and a suitable driving amplitude was selected to give a rms amplitude of around 0.5V before engaging.

Results and Discussion

Observation of Catalytically Driven Autonomous Movement. In aqueous hydrogen peroxide solutions, the motion of Pt/Au rods is visibly non-Brownian as they move in the direction of their long axis (Figure 1, also videos in Supporting Informa-

(6) Martin, B. R.; Dermody, D. J.; Reiss, B. D.; Fang, M.; Lyon, L. A.; Natan, M. J.; Mallouk, T. E. *Adv. Mater.* **1999**, *11*, 1021−1025.

(7) Morris, N. D.; Mallouk, T. E. *J. Am. Chem. Soc.* **2002**, *124*, 11114−11121.

Table 1. Diffusion Coefficients (in $\mu m^2/s$) for 2 μm Long Platinum/Gold Rods

	sampling interval (seconds)						
experiment	0.1	0.2	0.3	0.4	0.5	1.0	15
Au in H_2O[a]							0.41
Pt/Au in H_2O	0.43	0.41	0.40	0.40	0.39	0.42	
Pt/Au in H_2O_2[b]	4.13	6.61	9.41	11.6	13.8	23.7	

[a] From ref 11. [b] In 3.3% hydrogen peroxide.

tion) with *the platinum end forward*. A control experiment using three-striped (Au/Pt/Au) rods—which catalyze the decomposition of H_2O_2 at a similar rate—established that the asymmetric Pt/Au geometry was necessary for rapid axial movement. The average instantaneous speed of the catalytically powered Pt/Au rods is on the order of 8 μm/s, and they appear strikingly similar in both size and speed to multiflagellar bacteria[8] (which have average lengths and speeds of about 4 μm and 8 μm/s, respectively) when the latter are imaged in water. Movement in the axial direction is preferred for rod-shaped objects because the drag force is minimized in this direction.[9,10] Although the reaction proceeds with the formation of oxygen, bubbles (on the order of $d > 5$ μm) were observed few and far between and did not obscure our view of moving rods over short (<15 min) experiment times. The direction of movement of the rods is in contrast to the Whitesides experiment[3] in which the platinum "motor" is at the trailing end of the macroscopic moving objects (still image and video in Supporting Information).

The observed rod movement can be expressed in terms of diffusion coefficients or center-to-center displacement speeds. Diffusion coefficients were determined experimentally using trajectory diffusion methods and the two-dimensional diffusion coefficient is defined as $D = \langle d^2 \rangle / 4t$, where d is the center to center displacement in the time interval t. At time scales larger than the velocity relaxation time for the rods ($>10^{-5}$ s) the diffusion coefficient associated with Brownian motion is independent of the time interval. In pure water, rod movement is Brownian in nature and diffusion coefficients for rods obtained by trajectory analysis are similar to those reported previously (Table 1).[11] Diffusion coefficients obtained for platinum/gold rods in aqueous hydrogen peroxide are notably different from those obtained for the same rods in pure water or gold rods in aqueous hydrogen peroxide and depend on the duration of the sampling interval.

Analyzing motility using center-to-center displacement speeds requires the use of a directionality factor, which we define as the cosine of the angle between the rod axis and the direction that it moves (Figure 2). Thus, a rod that moves in the axial direction toward the platinum end has a directionality of 1 (cos 0), whereas rods moving perpendicular to the axial direction or backward have directionalities of 0 and −1, respectively. The product of the directionality and speed yields the velocity component along the rod axis, v_z. The Brownian component of translational velocity should become less important as the propulsive component increases, so that directionality increases from 0 to a value approaching 1, as shown in Figure 3. In pure water, the directionality is close to zero, as is expected of particles undergoing pure Brownian motion. As shown in Table 2, the directionality and speed both increase with increasing hydrogen peroxide concentration and begin to level off between 3.3% and 5% hydrogen peroxide. For comparison, the average v_z values for 2 μm pure gold and platinum rods at 3.3% hydrogen peroxide concentration were 0.5 and 2.7 μm/s, respectively. The movement of the platinum rods can be attributed to asymmetry in the rod geometry. From SEM image analysis, it appears that each template-grown rod has a concave end and a convex end. The rougher concave end has higher platinum surface area, resulting in more oxygen generation compared to the convex end.

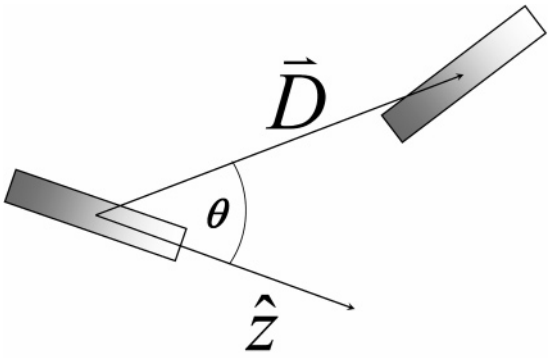

Figure 2. $\vec{D}$ gives the displacement of the rod over one time interval ($\Delta t = 0.1$ s). The directionality is defined by $cos(\theta)$, where θ is the initial angle between the rod axis ($\hat{z}$) and the displacement vector ($\vec{D}$). The axial velocity, $v_z = \vec{D} \cdot \hat{z}/\Delta t = \vec{D}/\Delta t \cos(\theta)$.

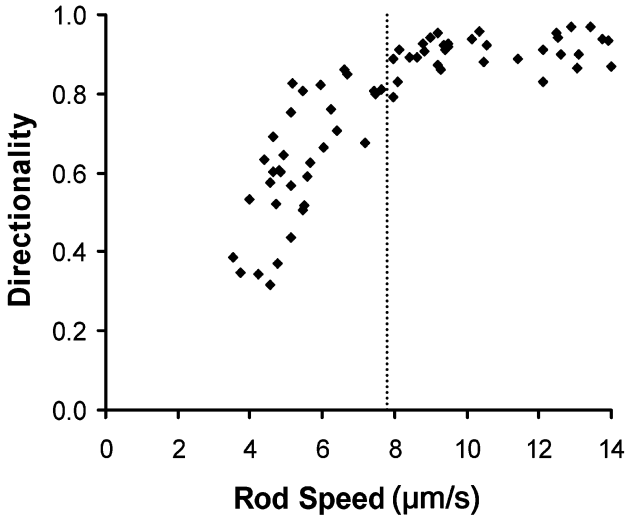

Figure 3. Relationship between speed and directionality for the 2 μm long platinum/gold rods in 3.3% aqueous H_2O_2. Dashed line represents average rod speed.

Table 2. Effect of Aqueous H_2O_2 Concentration on the Movement of 2 μm Platinum/Gold Rods[a]

H_2O_2 (wt. %)	speed (μm/s)[b]	directionality	v_z (μm/s)[b]
4.9	7.7 ± 0.9	0.78	6.6 ± 1.0
3.3	7.9 ± 0.7	0.75	6.6 ± 0.7
1.6	5.6 ± 0.6	0.65	4.0 ± 0.8
0.33	4.9 ± 0.3	0.60	3.4 ± 0.4
0.031	3.9 ± 0.5	0.19	0.9 ± 0.4
pure water	3.7 ± 0.3	0.07	0.4 ± 0.1

[a] Concentration of rods: 3.3×10^7 rods/mL. [b] Error limits represent 90% confidence intervals.

(8) *Bacillus cereus* from the Blake Peterson laboratory at Penn State.
(9) Perrin, F. *J. Phys. Radium* **1934**, *5*, 497−511.
(10) Probstein, R. F. *Physicochemical Hydrodynamics*; Butterworth: Boston, 1989; pp 109−112.
(11) St. Angelo, S. K.; Waraksa, C. C.; Mallouk, T. E. *Adv. Mater.* **2003**, *15*, 400−402.

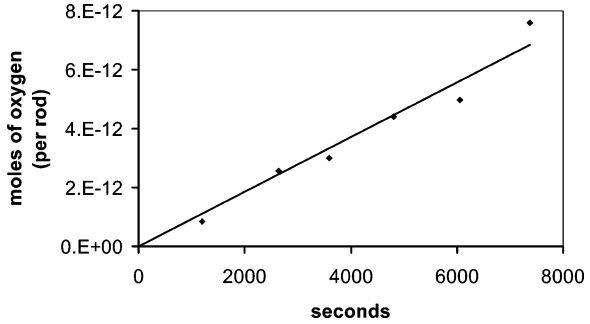

Figure 4. Oxygen evolution vs time for a suspension of Au/Pt rods in 3.7% aqueous H_2O_2.

The speed of moving rods varies with the hydrogen peroxide concentration, which suggests a relationship between rod speed and reaction rate. This relationship was confirmed by monitoring the rate at which oxygen is evolved from samples containing different concentrations of hydrogen peroxide and platinum/gold rods via gas chromatography (Figure 4). The experimental rate of oxygen formation from 3.7% hydrogen peroxide was found to be approximately 1/2000 of the limit imposed by the hydrogen peroxide diffusion rate. Thus, the rate of oxygen formation is limited by the turnover rate of the catalyst which, in turn, depends on the surface area of the platinum segment. Otherwise identical batches of rods grown at different plating potentials had different average velocities in hydrogen peroxide solutions, consistent with this hypothesis.

Interfacial Tension Model. We have considered several possible mechanisms for the motion of platinum/gold rods in hydrogen peroxide solutions. "Jet propulsion" mechanisms, in which oxygen generated at platinum impels the rod through a pressure increase or by momentum recoil of bursting bubbles, as in the Whitesides system, would propel a rod *away from* its platinum end. Diffusiophoretic transport models of colloidal particles in a gradient of neutral solute[12,13] (i.e., oxygen molecules) also predicts movement *away from* its platinum end with a velocity orders of magnitude slower than that observed experimentally.

The possibility of an interfacial tension gradient, which may be imposed by either a temperature or solute gradient, offers another alternative. Both temperature and chemical gradients are present in our system due to the exothermic decomposition of hydrogen peroxide. Because the platinum end is the source of these gradients, they are continually re-established as a rod moves through solution so long as hydrogen peroxide is present.

We can calculate the interfacial tension force created by the solute gradient by solving the convection-diffusion equation in the frame of the moving rod. The reaction establishes a concentration gradient of both hydrogen peroxide and oxygen along the length of the rod. Because H_2O_2 has almost the same interfacial tension as water,[14] oxygen is the only important solute in the calculation. Oxygen is a nonpolar molecule that cannot act as a hydrogen bond donor, and it thus disrupts the hydrogen bonding network of liquid water. We make the simplification that the liquid−solid interfacial tension gradient is directly proportional to the gradient in the mole fraction of oxygen in the solution. Although the calculated force does not vary much

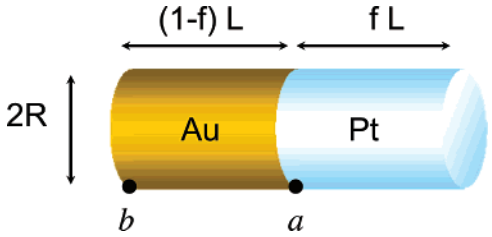

Figure 5. Schematic diagram of a Pt/Au nanorod showing the dimensions used in the calculation of interfacial forces.

if different functional forms are used, the linear model is consistent with data compiled by Acree for a variety of solute−solvent systems.[15]

To calculate the interfacial forces, we consider a rod with the dimensions shown in Figure 5. The concentration of oxygen (C) in the reference frame co-moving with the rod is obtained by solving the convection-diffusion eq 1:

$$\frac{\partial C}{\partial t} = -v \cdot \nabla C + D\nabla^2 C \qquad (1)$$

in which the first term corresponds to convection and the second to diffusion. Since the time needed to convect (or diffuse) a distance d is d/v (or d^2/D), the observed velocity of several microns per second together with $D \approx 10^{-5}$ cm^2/s imply that diffusion dominates out to a distance of order $D/v \approx 10^2$ μm. Thus, oxygen molecules are transported primarily by diffusion, which is not subject to the no-slip boundary condition that applies to convection. That is, we may treat the concentration field in the co-moving frame as constant in time and solve the steady-state diffusion equation $\nabla^2 C(r) = 0$ (Laplace equation) in the region outside the rod. The uniform flux of oxygen S (i.e., the surface area-normalized oxygen generation rate) into the fluid along the Pt surface and zero flux along the Au surface provide boundary conditions. This kind of time-independent diffusion problem is a familiar one in electrochemical systems, for example in deriving expressions for the steady-state current at microwire electrodes.[16]

We now make two simplifications: First, the rate of O_2 production is distributed uniformly over the curved part of the Pt surface, and the rate at the flat end is zero (the endcap area is only about one tenth of the total Pt area). Second, we assume that the rod is permeable to O_2, with the same diffusion coefficient as in water. Although the second approximation is not physically realistic, the volume of the rod is very small compared to the volume of solution within the diffusion length on the time scale of motion.

With these approximations, the problem can be solved by integrating the contributions of a continuum of point sources spread on the cylindrical Pt surface. Since the steady-state concentration around such a point source is the production rate times $1/(4\pi Dr)$, we obtain eq 2:

$$C(r) \approx \frac{S}{4\pi D}\int_{Pt} \frac{d^2 r'}{|r - r'|} \qquad (2)$$

Only the difference in concentration between the Pt/Au juncture and the extreme end of the Au part of the rod (points labeled *a*

(12) Anderson, J. L. *Annu. Rev. Fluid. Mech.* **1989**, *21*, 61−99.
(13) Staffeld, P. O.; Quinn, J. A. *J. Colloid Interface Sci.* **1989**, *130*, 88−100.
(14) Phibbs, M. K.; Giguere, P. A. *Can. J. Chem.* **1951**, *29*, 173−181.
(15) Acree, W. E., *J. Colloid Interface Sci.* **1984**, *101*, 575−576.
(16) Fulian, Q.; Gooch, K. A.; Fisher, A. C.; Stephens, N. P. G.; Compton, R. G. *Anal. Chem.* **2000**, *72*, 3480−3485. (b) Stephens, N. P. C.; Fulian, Q.; Gooch, K. A.; Fisher, A. C. *J. Phys. Chem. B* **2000**, *104*, 7110−7114.

and *b* in Figure 5) is needed to compute the force resulting from an interfacial tension gradient. Adopting cylindrical coordinates with point *a* as $z = 0$ and $\theta = 0$, the concentration at point *a* can be written as eq 3

$$C(a) \approx \frac{S}{4\pi D}\int_0^{fL}\int_0^{2\pi}\frac{Rd\theta dz}{\sqrt{2R^2(1-\cos\theta)+z^2}} \quad (3)$$

Now, for $z \gg R$, the integrand is close to 1/z so that the integral is essentially logarithmic and can be approximated by eq 4.

$$C(a) \approx \frac{SR}{2D}\ln(2fL/R) \quad (4)$$

The same procedure can be applied for *b*, as shown in eq 5.

$$C(b) = \frac{S}{4\pi D}\int_{(1-f)L}^{L}\int_0^{2\pi}\frac{Rd\theta dz}{\sqrt{2R^2(1-\cos\theta)+z^2}} \approx -\frac{SR}{2D}\ln(1-f) \quad (5)$$

Combining these last two results, we obtain the concentration difference ΔC.

$$\Delta C = C(a) - C(b) \approx \frac{SR}{2D}\ln(2f(1-f)L/R) \quad (6)$$

The approximation is asymptotically exact as the aspect ratio *L/R* becomes large. Conversely, the accuracy will deteriorate if the aspect ratio of the entire rod, or of either portion of the rod, becomes too small. In the case of the rods considered here, *L/R* is large and the results obtained with these approximations are within about 20% of those obtained by a more precise numerical solution using finite difference methods.

To calculate the force created by this concentration gradient, we must relate ΔC to the interfacial tension difference at points *a* and *b*. We begin by using Acree's observation[15] that the interfacial tension of a solution may be taken as the mole fraction-weighted average of the component interfacial tensions, eq 7.

$$\gamma_{(\text{solution})/X} = \sum_i \chi_i \gamma_{i/X} \quad (7)$$

In this equation, *X* represents the contacting phase (solid or vapor), and the sum is carried out over the *i* components of the solution. We note that $\gamma_{H2O2/X}$ is close to $\gamma_{H2O/X}$,[14] and therefore eq 7 may be written as eq 8.

$$\gamma_{(\text{solution})/X} = \chi_{O2}\gamma_{O2/X} + (1-\chi_{O2})\gamma_{H2O/X} \quad (8)$$

For X = vapor, $\gamma_{O2/X}$ is approximately zero and therefore $\gamma_{\text{solution}/X} \approx \chi_{H2O}\gamma_{H2O/X}$. To obtain the solution/Au interfacial tension, we can use Young's eq 9:

$$\gamma_{\text{vapor/Au}} - \gamma_{\text{solution/Au}} = \cos(\theta)\gamma_{\text{solution/vapor}} \quad (9)$$

Now taking $\gamma_{\text{solution/vapor}} \approx \chi_{H2O}\gamma_{H2O/\text{vapor}}$, and differentiating eq 9 with respect to χ_{H2O}, we obtain eq 10:

$$\frac{d\gamma_{\text{solution/Au}}}{d\chi_{H2O}} = -[H_2O]\frac{d\gamma_{\text{solution/Au}}}{dC} \approx -\cos(\theta)\gamma_{H2O/\text{vapor}} \quad (10)$$

Combining eqs 6 and 10 for the case where $f = 1/2$ (equal Au and Pt segments), and taking $\cos(\theta) = 1$ for a hydrophilic Au surface, we obtain the force on the rod

$$F = -2\pi R\frac{d\gamma_{\text{solution/Au}}}{dC}\Delta C \approx -\frac{S}{D}\pi R^2\frac{\gamma_{H2O/\text{vapor}}}{[H_2O]}\ln\left(\frac{L}{2R}\right) \quad (11)$$

The steady-state velocity (v) can be obtained by equating this force to the drag force eq 12 on the

$$F_{\text{drag}} = -\frac{2\pi\mu L v}{\ln(2L/R) - 0.72} \quad (12)$$

cylindrical rod.[17] Here μ is the viscosity of the fluid. By combining eq 11 and eq 12 we obtain from eq 13

$$v \approx \frac{SR^2\gamma}{2\mu DL[H_2O]}\ln\left(\frac{L}{2R}\right)\left[\ln\left(\frac{2L}{R}\right) - 0.72\right] \quad (13)$$

$v = 17$ μm/s for 2 μm long Pt/Au rods in 3.7% aqueous H_2O_2 solution, in which $\gamma_{H2O/\text{vapor}}$ is 72.0 mN/m, $[H_2O]$ is 55 M, and the measured oxygen evolution rate *S* is 8.4×10^{-8} mol/cm^{2}s. This derived value is in good agreement with the measured rod velocities of 4−18 μm/s in this medium.

Equation 13 may be simplified by noting that the two logarithmic terms vary slowly with *L* and *R*. This gives eq 14, which may be used to predict the scaling of the rod velocity with different

$$v \propto \frac{SR^2\gamma}{\mu DL} \quad (14)$$

parameters (*S*, *R*, *L*, γ, μ, *D*). Scaling experiments support the predicted strong dependence of the velocity on the rod radius *R*. 100 nm diameter Pt/Au rods showed only Brownian movement of the particles in 3.3% H_2O_2, and experiments with longer rods gave slower axial motion. By adding ethanol or surfactants to the solution, the liquid/vapor interfacial tension is lowered and the rod velocity decreases. Figure 6 shows a plot of average velocity vs the product $S\gamma$ for a sample of Pt/

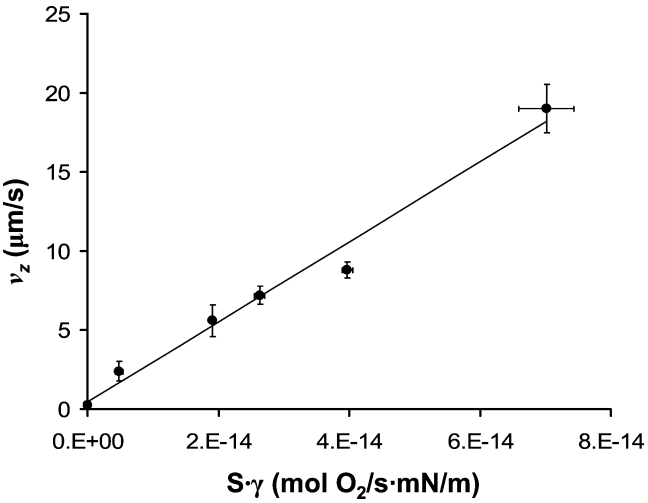

Figure 6. Effect of ethanol on axial velocity, v_z, where v_z is plotted versus the product of oxygen evolution rate per rod and solution surface tension (i.e., $S{\cdot}\gamma$). Included is a data point for rods moving in pure water, where the oxygen evolution rate is taken to be zero.

(17) Happel, J.; Brenner, H. Low Reynolds Number Hydrodynamics; Prentice Hall: Englewood Cliffs, NJ, 1965; eq 5−11.52.

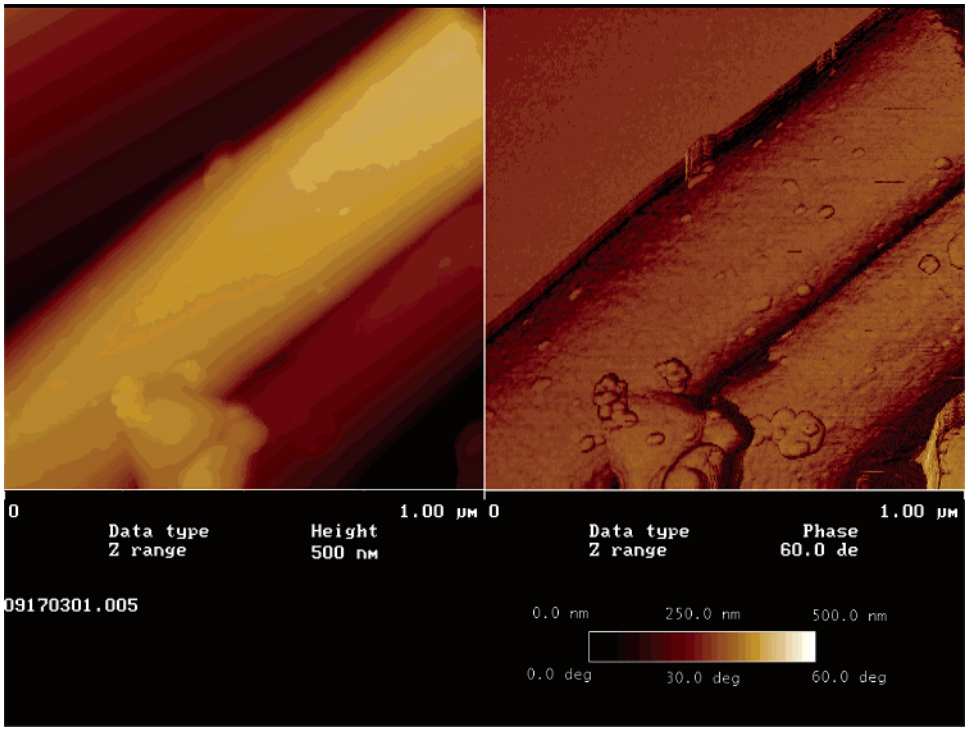

Figure 7. Tapping mode AFM topography (left) and phase shift (right) images of Pt/Au nanorods in air.

Au rods in ethanol−water solutions containing hydrogen peroxide. The plot is linear, as expected from eq 14. The addition of ethanol also affects μ and D, but according to the Stokes−Einstein equation the product of these two parameters is approximately constant, and thus these two effects balance each other. The linear dependence of v on $S\gamma$ provides strong evidence that the interfacial tension gradient is the dominant contributor to the movement of the rods.

Direction of Rod Motion. The calculation of the interfacial tension gradient above gives the correct magnitude of the force on the rods, as well as their steady-state velocity. It also correctly predicts the linear dependence of the force on the product $S\gamma$. An issue that is less straightforward to address is the observed direction of motion, which is toward the Pt end of the rod. Oxygen in an aqueous solution disrupts hydrogen bonding, and it therefore reduces the liquid/vapor interfacial tension. However, the relevant interfacial tension is at the gold surface, where the gradient exists (the interfacial tension is constant over the Pt surface, which is generating oxygen at a constant rate). If the gold surface is very polar, then the liquid/*solid* interfacial tension should actually *increase* as the oxygen concentration increases. This should result in motion toward the gold end, because the total free energy will be lowered by moving the polar gold surface into the more polar pure water. On the other hand, movement toward the platinum end will occur if the gold surface is hydrophobic, for example if it is covered with a vapor. In this case, the relevant interfacial tension is liquid/vapor.

Surfaces exposed to near-saturation levels of gaseous solutes in aqueous solutions are known to be covered by nanobubbles.[18] A recent report shows that even unmodified gold surfaces are partially covered by nanobubbles in air-saturated aqueous solutions.[19] In the context of our experiments, this is important in rationalizing the direction of motion of the nanorods. We have carried out tapping-mode atomic force microscopy (AFM) studies on Au/Pt nanorods to verify the presence of nanobubbles. Rods imaged in air (Figure 7) have relatively featureless phase images. Rods imaged under air-saturated water are dotted with 10−50 nm diameter features that show a negative phase shift (darker regions in Figure 8) relative to the background. These images were obtained under tapping conditions where the ratio between set-point tapping amplitude (A_{sp}) and the free amplitude (A_0) was 0.68. A combined theoretical/experimental study on polymer films by Magonov et al.[20] shows that at moderate tapping ($A_{sp}/A_0 \approx 0.4-0.7$), more negative phase shift corresponds to softer regions of the surface. Thus, the observed phase shift is consistent with identification of the dark features in the phase images as nanobubbles. Similar features were also observed on unmodified silicon surfaces in air-saturated water, which look very smooth when imaged in air. However, fresh mica surfaces appear smooth in water as well as in air. This is consistent with earlier reports[18] that nanobubbles tend to form on rough and hydrophobic surfaces, but not on smooth, hydrophilic surfaces. It also excludes the possibility that these features come from the influence of the liquid-tip interaction.

We were unable to obtain AFM images under conditions of hydrogen peroxide decomposition because of gas evolution in the sample cell. It is important to note that the steady-state concentration of oxygen at the Pt tip, which is on the order of 1 mM, is approximately equal to the maximum solubility of oxygen in water. It is therefore very likely that nanobubble coverage of the rod surface is at least as high as it is in air-saturated water (Figure 8). Because of the presence of nanobubbles, two distinct interfacial tensions enter into the calcula-

(18) Yang, J.; Duan, J.; Fornasiero, D.; Ralston, J. *J. Phys. Chem. B* **2003**, *107*, 6139−6147.

(19) Holmberg, M.; Kuhle, A.; Garnaes, J.; Morch, K. A.; Boisen, A. *Langmuir* **2003**, *19*, 10510−10513.

(20) Magonov, S. N.; Elings, V.; Whangbo, M.-H. *Surf. Sci.* **1997**, *375*, L385−L391.

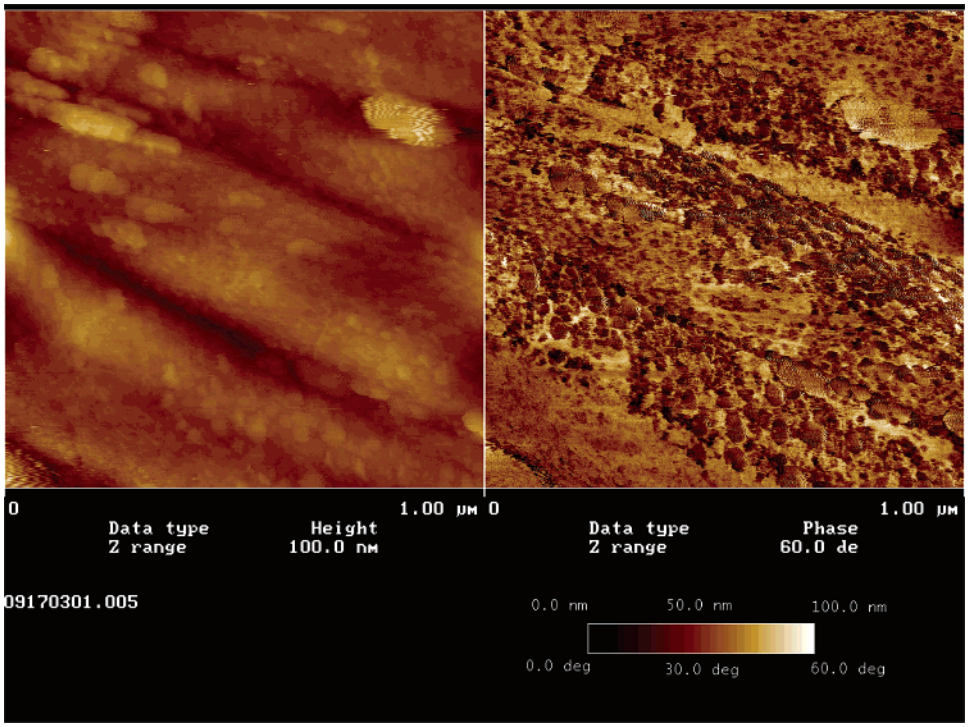

Figure 8. Tapping mode AFM topography (left) and phase shift (right) images of Pt/Au nanorods in air-saturated water.

tion of the net force on the nanorod: the interface between bare gold and the solution, and the interface between an oxygen nanobubble and the solution. The nanobubble-derived force scales with $\gamma_{\text{solution/vapor}}$, whereas the remaining contribution scales with $\gamma_{\text{solution/Au}} - \gamma_{\text{vapor/Au}}$. However, Young's eq 9 for the vapor-Au-solution three-phase boundary equates ($\gamma_{\text{vapor/Au}} - \gamma_{\text{solution/Au}}$) with $cos(\theta)\gamma_{\text{solution/vapor}}$. Therefore, both contributions scale with $\gamma_{\text{solution/vapor}}$. The resulting dependence of the rod interfacial tension on the water mole fraction is thus given by eq 15, which corrects eq 10 for partial coverage by nanobubbles

$$\frac{d\gamma_{\text{solution/rod}}}{d\chi_{\text{H2O}}} = (A - (1 - A)\cos(\theta))\gamma_{\text{H2O/vapor}} \qquad (15)$$

In this equation, A is the fraction of the Au surface that is occupied by nanobubbles. The nanobubble coverage is not known precisely under conditions of hydrogen peroxide decomposition, but A should be sizable judging from AFM images acquired in air-saturated water (Figure 8). Taking $A \approx 1$ and $\cos(\theta) \approx 1$, we obtain the same force given in eq 11, but with motion directed toward the Pt end of the rod.

Alternative Gradient Forces. It is important to note that while other effects such as local heating could contribute to rod movement, the calculated interfacial tension force is sufficient to account for our observations; to put it another way, if other mechanisms are operative, they must approximately cancel each other for the observed velocity to match that calculated from the interfacial tension force alone.

We can calculate the forces created by two possible effects (surface tension lowering and pressure generation) of heat evolved in the H_2O_2 decomposition reaction. First, like oxygen, heat diffuses, leading to a temperature gradient along the rod, and therefore an additional surface tension gradient since the surface tension is temperature-dependent. The ratio of forces arising from the temperature gradient to that arising from the oxygen concentration gradient is easily calculated, because the similar equations describe the profiles of oxygen concentration ($\nabla^2 C(r) = 0$) and temperature ($s^2 T(r) = 0$). We can write

$$\frac{T - \text{gradient force}}{[O_2] - \text{gradient force}} = \frac{S_\epsilon}{S_{\text{O2}}} \frac{D_{\text{O2}}}{\kappa} \frac{d\gamma/dT}{d\gamma/dC} \qquad (16)$$

where the thermal conductivity of water $\kappa = 6 \times 10^{-1}$ W/K m, $d\gamma/dT \approx 1.5 \times 10^{-4}$ N/K m, and S_ϵ/S_{O2}, the exothermicity of the reaction, is 190 kJ/mol. These values lead to a temperature gradient induced force that is roughly 2% of the concentration gradient induced force, and even this small ratio is probably an overestimate because the metallic rod itself has a higher thermal conductivity than water.

Second, heating of the fluid near the Pt end of the rod increases the pressure there, which tends to push the rod toward the Au end (opposite to the observed direction of motion). The pressure increase is a result of hindered thermal expansion, so the speed with which the pressure can propel the rod is considerably overestimated by supposing that the full isobaric thermal expansion is accommodated by the motion of the rod. The thermal energy evolved per second by one rod is $Q = 2 \times 10^{-11}$ J, the coefficient of thermal expansion at room temperature is $\alpha = 3 \times 10^{-4}$ K^{-1}, and the heat capacity by volume is $c = 4 \times 10^{-12}$ J/K μm^3. The maximum increase in volume is therefore $\Delta V = (\alpha/c)Q = 6 \times 10^{-3}$ μm^3. Since the cross-sectional area of a rod is 0.1 μm^2, this can only produce a speed less than 0.06 μm/s.

Conclusions

We have shown that it is possible to power the motion of nanoscale and microscale objects by using catalytic reactions. The observed velocities of the platinum/gold nanorods are comparable to those of flagellar bacteria and similar living

organisms: approximately 2−10 body lengths per second. The force that propels these rods arises from an interfacial tension gradient that is continuously re-established as the rod moves, and in this way the mechanism of movement is quite different from that of macroscale objects propelled by the same catalytic reaction. There is a very large number of metals, metal derivatives, and enzymes that catalyze reactions, which can in principle be used to generate gradient-based forces. By appropriate design, these forces can be translated into anisotropic surface forces. Depending on the shape of the object and the placement of the catalyst, different kinds of motion from linear (e.g., Figure 1) to rotational could be achieved. The nano/microengines could, in turn, be tethered or coupled to other objects in spatially defined ways using a variety of known techniques to create a whole new class of catalytically powered nano/micromachines.

Acknowledgment. We thank Dr. Nina Kovtukhova for technical assistance. The work was funded by the National Science Foundation under Grants DMR 0080019 and DMR 0213623 (A.S., V.H.C.) and by the Office of Naval Research/Defense Advanced Research Projects Agency (T.E.M.).

Supporting Information Available: Two videos of 2 μm long Pt/Au rods in pure water and 2.5% hydrogen peroxide, a video of Au/Pt/Au rods in 2.5% hydrogen peroxide, and a video of a long Pt/Au rod with a color still photo of the same rod, showing that the direction of motion is toward the Pt end. This material is available free of charge via the Internet at http://pubs.acs.org.

JA047697Z